

Non-Fermi liquid behavior at the onset of incommensurate $2k_F$ charge or spin density wave order in two dimensions

Tobias Holder¹ and Walter Metzner¹

¹Max Planck Institute for Solid State Research, D-70569 Stuttgart, Germany

(Dated: April 4, 2024)

We analyze the influence of quantum critical fluctuations on single-particle excitations at the onset of incommensurate $2k_F$ charge or spin density wave order in two-dimensional metals. The case of a single pair of hot spots at high symmetry positions on the Fermi surface needs to be distinguished from the case of two hot spot pairs. We compute the fluctuation propagator and the electronic self-energy perturbatively in leading order. The energy dependence of the single-particle decay rate at the hot spots obeys non-Fermi liquid power laws, with an exponent $2/3$ in the case of a single hot spot pair, and exponent one for two hot spot pairs. The prefactors of the linear behavior obtained in the latter case are not particle-hole symmetric.

PACS numbers: 71.10.Hf, 75.30.Fv, 64.70.Tg

Charge and spin correlations in metals exhibit a well-known singularity at wave vectors that connect points on the Fermi surface with antiparallel Fermi velocities. The singularity is caused by an enhanced phase space for low-energy particle-hole excitations near such wave vectors. It leads, among other effects, to the Kohn anomaly [1] in phonon spectra and to the long-ranged RKKY interaction between magnetic impurities in metals [2]. For isotropic Fermi surfaces the singularity is located at wave vectors with modulus $2k_F$, where k_F is the radius of the Fermi surface. In inversion symmetric crystalline solids, singular wave vectors are given by the condition

$$\xi_{(\mathbf{Q}+\mathbf{G})/2} = 0, \quad (1)$$

where $\xi_{\mathbf{k}} = \epsilon_{\mathbf{k}} - \mu$ is the single-particle excitation energy, and \mathbf{G} is a reciprocal lattice vector. Eq. (1) is the lattice generalization of the condition $|\mathbf{Q}| = 2k_F$ for isotropic systems. Hence, we generally refer to wave vectors satisfying that condition as $2k_F$ vectors.

$2k_F$ singularities are more pronounced in systems with reduced dimensionality. Charge and spin correlations in low dimensional systems are often peaked at $2k_F$ vectors, such that they are privileged wave vectors for charge and spin density wave instabilities. $2k_F$ instabilities are ubiquitous in (quasi) one-dimensional electron systems [3]. Here we focus on *two-dimensional* systems, where $2k_F$ instabilities also play an important role. In particular, the ground state of the two-dimensional Hubbard model exhibits a spin density wave instability at a $2k_F$ vector, at least at weak coupling [4, 5]. Furthermore, spatially modulated nematic order, that is, *d*-wave bond charge order, occurs preferably at $2k_F$ vectors [6]. For Fermi surfaces crossing the antiferromagnetic zone boundary, the highest peaks in the *d*-wave charge response are at $2k_F$ vectors connecting magnetic hot spots, such that the bond order instability can be triggered by antiferromagnetic interactions [7, 8].

In this paper we analyze consequences of quantum criticality at the onset of *incommensurate* $2k_F$ charge or spin

density wave order in the ground state, in cases where the phase transition (e.g., as a function of electron density) is continuous. The momentum and energy dependences of the $2k_F$ fluctuation propagator differs strongly from that for generic incommensurate wave vectors [9], and also from the one for commensurate (π, π) charge or spin density wave instabilities [10, 11], for which quantum critical properties have been extensively studied [7, 12]. The quantum critical behavior at $2k_F$ density wave transitions in two dimensional metals was addressed many years ago by Altshuler et al. [13], who computed several properties for the case that the $2k_F$ vector is half a reciprocal lattice vector. The special case where (π, π) is a $2k_F$ vector was recently revisited, and qualitative modifications due to additional umklapp processes were revealed [14]. For incommensurate $2k_F$ vectors, Altshuler et al. found strong infrared divergencies and concluded that fluctuations destroy the quantum critical point (QCP), such that the phase transition is ultimately discontinuous.

In the following we will analyze the influence of incommensurate $2k_F$ quantum critical fluctuations on single-particle excitations by computing the electronic self-energy at $2k_F$ hot spots [15] on the Fermi surface to first order (one loop) in the fluctuation propagator. We will show that one needs to distinguish the case where the $2k_F$ vector connects only one pair of hot spots at high symmetry points from cases where it connects two hot spot pairs. Only the former case was considered in Ref. [13]. In both cases, the quasi-particle decay rate obeys non-Fermi liquid power laws as a function of energy, but with distinct exponents, $2/3$ and one, respectively. These power laws may be observed in a certain energy window even in case that the fluctuations are ultimately cut off by a first order transition, or by a secondary instability in close vicinity of the QCP.

To compute the electronic self-energy, we first need to derive the momentum and energy dependence of the effective interaction (fluctuation propagator) at the QCP.

At leading order, the latter is given by the RPA expression $D(\mathbf{q}, \omega) = g[1 - g\Pi_0(\mathbf{q}, \omega)]^{-1}$, where g is the coupling parametrizing the bare interaction in the instability channel, and Π_0 is the bare polarization function of the system. The RPA effective interaction and the one-loop self-energy are not affected qualitatively by details such as the spin structure and form factors (s -wave, d -wave, etc.) in $\Pi_0(\mathbf{q}, \omega)$. Finite renormalizations from non-critical fluctuations could be incorporated by using a renormalized coupling and a reduced quasi-particle weight.

At the onset of density wave order, $g\Pi_0(\mathbf{Q}, 0)$ is equal to one such that the effective interaction diverges. The momentum and energy dependence of $D(\mathbf{q}, \omega)$ at that point is obtained by expanding $\Pi_0(\mathbf{q}, \omega)$ for \mathbf{q} near \mathbf{Q} and small energies. Here the $2k_F$ -singularity comes into play. The shape of that singularity can be deduced from the expanded analytic result [16] for $\Pi_0(\mathbf{q}, \omega)$ for fermions in the continuum with a parabolic dispersion $\epsilon_{\mathbf{k}} = \frac{\mathbf{k}^2}{2m}$,

$$\Pi_0(\mathbf{q}, \omega) = -\frac{m}{2\pi} + \frac{\sqrt{m}}{4\pi v_F} \times \left(\sqrt{e_{\mathbf{q}} + \omega + i0^+} + \sqrt{e_{\mathbf{q}} - \omega - i0^+} \right), \quad (2)$$

where $e_{\mathbf{q}} = v_F(|\mathbf{q}| - 2k_F)$, and v_F is the Fermi velocity. The complex roots are defined with a branch cut on the negative real axis. The infinitesimal imaginary parts under the roots specify that the real frequency (that is, energy) axis is approached from above. For electrons in a crystal, $\Pi_0(\mathbf{q}, \omega)$ is singular on the $2k_F$ -lines given by $\xi_{(\mathbf{q}+\mathbf{G})/2} = 0$. The momentum dependence is regular along these lines, but singular in perpendicular direction. To parametrize momenta near the instability vector \mathbf{Q} , we use normal and tangential coordinates q_r and q_t , respectively, as described in Fig. 1. The coordinate q_r

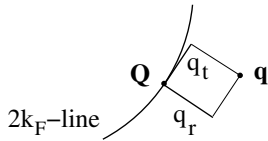


FIG. 1. Local coordinates q_r and q_t for momenta near \mathbf{Q} in the \mathbf{q} -plane.

is defined positive on the “outer” side of the $2k_F$ -line and negative on the “inner” side. The generalization of Eq. (2) for electrons in a crystal can then be written as

$$\Pi_0(\mathbf{q}, \omega) = \Pi_0(\mathbf{Q}, 0) + a \left(\sqrt{e_{\mathbf{q}} + \omega + i0^+} + \sqrt{e_{\mathbf{q}} - \omega - i0^+} \right) - b e_{\mathbf{q}} - c q_t \quad (3)$$

for \mathbf{q} near \mathbf{Q} and small ω , where a, b, c are constants and $e_{\mathbf{q}} = v_F q_r + \frac{q_t^2}{4m}$. Here v_F is the Fermi velocity at the Fermi points \mathbf{k}_F and $-\mathbf{k}_F$ connected by \mathbf{Q} , and the effective mass m parametrizes the curvature of the Fermi

surface at those points (mv_F is the radius of curvature). Note that $e_{\mathbf{q}}/v_F$ is the oriented distance of \mathbf{q} from the $2k_F$ -line in the \mathbf{q} -plane, defined positive outside and negative inside. The prefactor of the singularity a is fully determined by the Fermi velocity and curvature at $\pm\mathbf{k}_F$ as

$$a = N \frac{\sqrt{m}}{4\pi v_F}, \quad (4)$$

where N is the number of internal degrees of freedom such as spin. If Π_0 contains form factors, there may be a corresponding additional factor. The other constants b and c receive contributions from everywhere; b vanishes for a quadratic dispersion, but is otherwise typically positive; c vanishes for any isotropic dispersion, and also at symmetry points on the lattice, that is, for an axial or diagonal \mathbf{k}_F . Eq. (3) describes the singularity at $2k_F$ -vectors \mathbf{Q} connecting a single pair of hot spots on the Fermi surface. The more complicated but important case of $2k_F$ -vectors connecting two such pairs will be discussed below. Inserting Eq. (3) into the RPA expression for the effective interaction one obtains, at the QCP,

$$D(\mathbf{q}, \omega) = - \left[a \left(\sqrt{e_{\mathbf{q}} + \omega + i0^+} + \sqrt{e_{\mathbf{q}} - \omega - i0^+} \right) - b e_{\mathbf{q}} - c q_t \right]^{-1}. \quad (5)$$

Note that the coupling constant g has canceled out. The effective interaction diverges for $\mathbf{q} \rightarrow \mathbf{Q}$, $\omega \rightarrow 0$. The momentum and energy dependence of the singularity differs strongly from the one for density wave instabilities at generic (not $2k_F$) wave vectors [9–11].

The imaginary part of the one-loop self-energy for electrons coupled by a fluctuation propagator $D(\mathbf{q}, \omega)$ can generally be written as [17]

$$\text{Im}\Sigma(\mathbf{k}, \omega) = M \int \frac{d^d k}{(2\pi)^d} [b(\xi_{\mathbf{k}'} - \omega) + f(\xi_{\mathbf{k}'})] \times \text{Im}D(\mathbf{k}' - \mathbf{k}, \xi_{\mathbf{k}'} - \omega), \quad (6)$$

where b and f are the Bose and Fermi functions, respectively. The multiplicity factor M is one for charge fluctuations, and three for spin fluctuations. At zero temperature,

$$b(\xi_{\mathbf{k}'} - \omega) + f(\xi_{\mathbf{k}'}) = \begin{cases} -1 & \text{for } 0 < \xi_{\mathbf{k}'} < \omega, \\ 1 & \text{for } \omega < \xi_{\mathbf{k}'} < 0, \end{cases} \quad (7)$$

and otherwise 0. We now compute the low energy behavior of $\text{Im}\Sigma(\mathbf{k}_F, \omega)$ at hot spots \mathbf{k}_F on the Fermi surface.

$2k_F$ instabilities with a single pair of hot spots $\pm\mathbf{k}_F$ occur naturally at high symmetry points, that is, with \mathbf{k}_F and \mathbf{Q} in axial (see Fig. 2a) or diagonal direction. In these cases, the fluctuation propagator at the QCP is given by Eq. (5) with $c = 0$. For $\mathbf{k} = \mathbf{k}_F$ the dominant contributions to the integral in Eq. (6) come from momenta \mathbf{k}' near $-\mathbf{k}_F$. We assume that the Fermi surface is

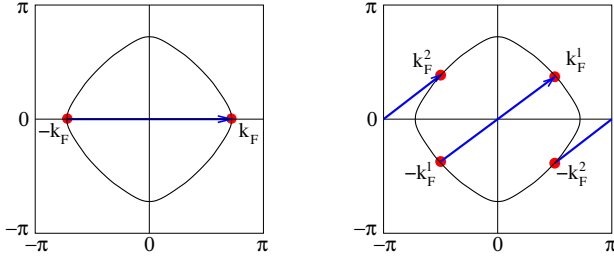


FIG. 2. (a) Axial $2k_F$ wave vector of the form $(Q, 0)$ and (b) $2k_F$ wave vector of the form (π, Q) , and the corresponding hot spots on the Fermi surface.

convex at $\pm \mathbf{k}_F$ in the following steps, but the final result is equally valid for a concave Fermi surface. Introducing normal and tangential coordinates for \mathbf{k}' near $-\mathbf{k}_F$, one can expand $\xi_{\mathbf{k}'} = v_F k'_r + \frac{k'^2_t}{2m}$ and $e_{\mathbf{k}'-\mathbf{k}_F} = v_F k'_r + \frac{k'^2_t}{4m}$. Substituting the integration variables k'_r and k'_t by the new variables $k' = -e_{\mathbf{k}'-\mathbf{k}_F}/v_F$ and $\omega' = \xi_{\mathbf{k}'}$, with the Jacobian $\sqrt{m}/\sqrt{\omega' + v_F k'}$, one obtains

$$\begin{aligned} \text{Im}\Sigma(\mathbf{k}_F, \omega) &= \frac{2Mv_F}{\pi N} \int_0^\omega d\omega' \int_{-\omega'/v_F}^\infty \frac{dk'}{\sqrt{\omega' + v_F k'}} \\ &\times \text{Im} \left[\sqrt{\omega' + i0^+ - \omega - v_F k'} \right. \\ &\left. + \sqrt{\omega - \omega' - i0^+ - v_F k'} + \bar{b}v_F k' \right]^{-1} \quad (8) \end{aligned}$$

for $\omega > 0$, and a similar expression for $\omega < 0$. The constant \bar{b} is given by

$$\bar{b} = b/a = \frac{4\pi v_F}{N\sqrt{m}} b. \quad (9)$$

For $\omega \rightarrow 0$, the integral in Eq. (8) is dominated by large momenta, $k' \gg (\omega - \omega')/v_F$, such that we can approximate $\sqrt{\omega' + i0^+ - \omega - v_F k'} + \sqrt{\omega - \omega' - i0^+ - v_F k'}$ by $i(\omega - \omega')/\sqrt{v_F k'}$. Substituting $k' = \omega \tilde{k}/v_F$, $\omega' = \omega \tilde{\omega}$, we obtain

$$\text{Im}\Sigma(\mathbf{k}_F, \omega) = \frac{2M\omega}{\pi N} \int_0^1 d\tilde{\omega} \int_{-\tilde{\omega}}^\infty \text{Im} \frac{d\tilde{k}}{i(1 - \tilde{\omega}) + \bar{b}\sqrt{\tilde{\omega}}\tilde{k}^{3/2}}. \quad (10)$$

The integral can now be computed analytically, yielding

$$\text{Im}\Sigma(\mathbf{k}_F, \omega) = -\frac{2M}{\sqrt{3}N} (|\omega|/\bar{b})^{2/3}, \quad (11)$$

which is valid also for $\omega < 0$. The self-energy at the hot spots thus exhibits a non-Fermi liquid power law behavior with an exponent $2/3$. The leading contributions come from energies $\omega' \sim \omega$, normal momenta $k'_r \sim |\omega|^{2/3}$, and tangential momenta $k'_t \sim |\omega|^{1/3}$. Remarkably, the same scaling behavior holds for nematic and U(1)-gauge quantum criticality [18–21], although the momentum and energy dependence of the fluctuation propagator is completely different.

We now turn to the second important case, where \mathbf{Q} connects two pairs of hot spots. This happens for spin density instabilities at wave vectors of the form $\mathbf{Q} = (\pi, Q)$ or (Q, π) , as found for example in Hartree-Fock calculations for the two-dimensional Hubbard model [4, 5]. The pairs of hot spots are located at $\pm(\frac{\pi}{2}, \frac{Q}{2})$ and $\pm(\frac{\pi}{2}, -\frac{Q}{2})$ in this case (Fig. 2b). Another example is provided by d -wave bond charge order at wave vectors of the form $\mathbf{Q} = (Q, Q)$ [6, 7]. The very fact that \mathbf{Q} connects two pairs of hot spots leads to peaks in the polarization function, such that density wave instabilities are favored at such special wave vectors. We now compute the singularity of the fluctuation propagator at the QCP and the energy dependence of the self-energy at hot spots for incommensurate density wave instabilities with two hot spot pairs. We present the calculation for the specific case $\mathbf{Q} = (\pi, Q)$ shown in Fig. 2b, while the result holds for the other cases, too.

The wave vector \mathbf{Q} is a crossing point of two $2k_F$ -lines. Hence, the $2k_F$ singularities on these lines have to be added, leading to

$$\Pi_0(\mathbf{q}, \omega) = \Pi_0(\mathbf{Q}, 0) + \sum_{n=1,2} a (\sqrt{e_{\mathbf{q}}^n + \omega} + \sqrt{e_{\mathbf{q}}^n - \omega}) - b e_{\mathbf{q}}^n, \quad (12)$$

where $e_{\mathbf{q}}^n/v_F$ is the oriented distance from the n -th $2k_F$ -line. We have suppressed the infinitesimal imaginary parts $i0^+$ to shorten the formula. We have also discarded the tangential momentum dependence (that is, $c = 0$) to simplify the expressions. It will become clear that this term affects only prefactors and can easily be reinstalled in the end. The fluctuation propagator at the QCP is then given by

$$D(\mathbf{q}, \omega) = - \left[\sum_{n=1,2} a (\sqrt{e_{\mathbf{q}}^n + \omega} + \sqrt{e_{\mathbf{q}}^n - \omega}) - b e_{\mathbf{q}}^n \right]^{-1}. \quad (13)$$

We now evaluate the one-loop self-energy at one of the hot spots, say \mathbf{k}_F^1 . It doesn't matter which hot spot we choose, because they are related by lattice symmetries. The integral in Eq. (6) is dominated by momenta \mathbf{k}' near $-\mathbf{k}_F^1$. Representing \mathbf{k}' by normal and tangential coordinates k'_r and k'_t , respectively, we can expand $\xi_{\mathbf{k}'} = v_F k'_r + \frac{k'^2_t}{2m}$ and $e_{\mathbf{k}'-\mathbf{k}_F^1} = v_F k'_r + \frac{k'^2_t}{4m}$ as in the case with only one hot spot pair. If the second $2k_F$ -line crosses the first one under an angle ϕ , one simply has to rotate the momentum variables to obtain

$$e_{\mathbf{k}'-\mathbf{k}_F}^2 = v_F (k'_r \cos \phi - k'_t \sin \phi) + \frac{(k'_t \cos \phi + k'_r \sin \phi)^2}{4m}. \quad (14)$$

Since the integral is again dominated by contributions with $|k'_r| \ll |k'_t|$, we can simplify this to $e_{\mathbf{k}'-\mathbf{k}_F}^2 = -v_F k'_t \sin \phi$. Changing integration variables to $k' =$

$-e_{\mathbf{k}'-\mathbf{k}_F}^1/v_F$ and $\omega' = \xi_{\mathbf{k}'}$, as previously, yields

$$\begin{aligned} \text{Im}\Sigma(\mathbf{k}_F^1, \omega) &= \frac{Mv_F}{N\pi} \int_0^\omega d\omega' \int_{-\omega'/v_F}^\infty \frac{dk'}{\sqrt{\omega' + v_F k'}} \\ &\times \sum_{k'_t = \pm 2\sqrt{m}\sqrt{\omega' + v_F k'}} \\ &\times \text{Im} \left[\left(\sqrt{\omega' - \omega - v_F k'} + \omega \leftrightarrow \omega' \right) + \bar{b}v_F k' \right. \\ &+ \left(\sqrt{\omega' - \omega - v_F k'_t \sin \phi} + \omega \leftrightarrow \omega' \right) \\ &\left. + \bar{b}v_F k'_t \sin \phi \right]^{-1} \end{aligned} \quad (15)$$

for $\omega > 0$. Contributions from $k'_t > 0$ dominate over those from $k'_t < 0$ for small ω . The first and the last term in the denominator is of order $\sqrt{\omega}$, while the second term is of order ω , and the third one is of order $\omega^{3/4}$ for $k'_t > 0$. Keeping only the leading terms, and substituting $k' = \tilde{\omega}\tilde{k}/v_F$, $\omega' = \omega\tilde{\omega}$, yields

$$\begin{aligned} \text{Im}\Sigma(\mathbf{k}_F^1, \omega) &= \frac{M\omega}{N\pi} \int_0^1 d\tilde{\omega} \int_{-\tilde{\omega}}^\infty \frac{d\tilde{k}}{\sqrt{\tilde{\omega} + \tilde{k}}} \\ &\times \text{Im} \left[\sqrt{\tilde{\omega} - 1 - \tilde{k}} + \sqrt{1 - \tilde{\omega} - \tilde{k}} \right. \\ &\left. + 2\bar{b}v_F \sin \phi \sqrt{m} \sqrt{\tilde{\omega} + \tilde{k}} \right]^{-1}. \end{aligned} \quad (16)$$

Using $\tilde{\kappa} = \tilde{\omega} + \tilde{k}$ and $\tilde{\omega}$ as integration variables, implementing also the case $\omega < 0$, and restoring the imaginary infinitesimals $i0^+$, we obtain the final result

$$\begin{aligned} \text{Im}\Sigma(\mathbf{k}_F^1, \omega) &= \frac{M\omega}{N\pi} \int_0^1 d\tilde{\omega} \int_0^\infty \frac{d\tilde{\kappa}}{\sqrt{\tilde{\kappa}}} \\ &\times \text{Im} \left[\sqrt{(2\tilde{\omega} - 1)\text{sgn}(\omega) + i0^+ - \tilde{\kappa}} \right. \\ &\left. + \sqrt{\text{sgn}(\omega) - i0^+ - \tilde{\kappa} + 2\tilde{b}\sqrt{\tilde{\kappa}}} \right]^{-1}, \end{aligned} \quad (17)$$

with the dimensionless constant

$$\tilde{b} = (v_F \sqrt{m} \sin \phi) \bar{b} = (4\pi N^{-1} v_F^2 \sin \phi) b. \quad (18)$$

The imaginary part of the self-energy is thus linear in ω at small ω , with a prefactor depending only on \tilde{b} . Note that \tilde{b} does not depend on the curvature of the Fermi surface at the hot spot. A striking feature is that the prefactor for $\omega > 0$ differs from the one for $\omega < 0$. For a convex Fermi surface, as assumed above, the prefactor for negative energies (holes) is larger than for positive energies (particles), and vice versa for a concave Fermi surface. For $\tilde{b} \gg 1$, Eq. 17 can be simplified to $\text{Im}\Sigma(\mathbf{k}_F^1, \omega) = -MN^{-1}C_\pm|\omega|$ with $C_+ = (\frac{1}{4} - \frac{1}{2\pi})\tilde{b}^{-1}$ and $C_- = (\frac{1}{4} + \frac{1}{2\pi})\tilde{b}^{-1}$, for $\omega > 0$ and $\omega < 0$, respectively. These asymptotic expressions provide a good approximation for $\tilde{b} \geq 10$.

Following the above derivation, one can see that including a tangential momentum dependence with a prefactor c as in Eq. (3) merely amounts to an additional

contribution proportional to k'_t in the denominator of Eq. (15), and subleading terms, so that \tilde{b} in Eq. (17) is replaced by $\tilde{b} - \tilde{c}$ with $\tilde{c} = 4\pi N^{-1} v_F (1 - \cos \phi) c$.

Let us pick the $2k_F$ spin-density wave instability obtained from Hartree-Fock studies of the two-dimensional Hubbard model [4, 5] as an example. In this case, the constants \tilde{b} and \tilde{c} can be determined by computing $\Pi_0(\mathbf{q}, 0)$ for \mathbf{q} near $\mathbf{Q} = (\pi, Q)$ and v_F explicitly from the tight-binding band structure. Typical values for \tilde{b} are between 10 and 20, while \tilde{c} is considerably smaller. The prefactor to the linear energy dependence of $\text{Im}\Sigma(\mathbf{k}_F^1, \omega)$ is thus about 0.05 for $\omega < 0$ and about 0.01 for $\omega > 0$.

For momenta away from the hot spots, the self-energy obeys Fermi liquid behavior in the low energy limit. Close to the hot spots, there is a crossover between the non-Fermi liquid power-laws derived above at intermediate energies, and Fermi liquid behavior at very low energies. For momenta on the Fermi surface at a small distance k_t from the next hot spot, the crossover scale ω^* is proportional to k_t^3 for the case of a single hot spot pair, and proportional to k_t^2 for two hot spot pairs.

We have computed the self-energy only to one-loop order. This suffices to detect the breakdown of Fermi liquid theory, but higher orders may modify the power-laws. For the intensively studied cases of commensurate antiferromagnetic and nematic quantum criticality, corrections to the one-loop power-laws have been found at two-loop [7] and three-loop order [21], respectively. Higher order terms may also destroy the QCP at low energy scales, and preempt it by a first order transition [13], or trigger another instability such as pairing.

In summary, we have analyzed the fate of single-particle excitations at the onset (QCP) of incommensurate $2k_F$ charge or spin density wave order in a two-dimensional metal. There are two qualitatively distinct important scenarios, namely those with a single pair of hot spots at high lattice symmetry positions, and cases with two hot spot pairs. The dynamical fluctuation propagator exhibits peculiar square root singularities in both cases. The energy dependence of the single-particle decay rate at the hot spots as obtained from the one-loop self-energy obeys non-Fermi liquid power laws, with an exponent $2/3$ in the case of a single hot spot pair, and exponent one for two hot spot pairs. The prefactors of the linear behavior obtained in the latter case exhibit a pronounced particle-hole asymmetry.

In future work one should analyze the role of higher order contributions in a suitable renormalization group framework. It will also be very interesting to extend the present analysis to the quantum critical regime at finite temperature, study transport properties, and relate the results to correlated electron compounds with $2k_F$ instabilities.

We are grateful to F. Benitez, A. Eberlein, and H. Yamase for valuable discussions.

-
- [1] W. Kohn, Phys. Rev. Lett. **2**, 393 (1959).
 - [2] M. A. Ruderman and C. Kittel, Phys. Rev. **96**, 99 (1954); T. Kasuya, Prog. Theor. Phys. **16**, 45 (1956); Y. Yoshida, Phys. Rev. **106**, 893 (1957).
 - [3] T. Giamarchi, *Quantum Physics in One Dimension* (Oxford University Press, Oxford, 2004).
 - [4] H. J. Schulz, Phys. Rev. Lett. **64**, 1445 (1990).
 - [5] P. A. Igoshev, M. A. Timirgazin, A. A. Katanin, A. K. Arzhnikov, and V. Yu. Irkhin, Phys. Rev. B **81**, 094407 (2010).
 - [6] T. Holder and W. Metzner, Phys. Rev. B **85**, 165130 (2012).
 - [7] M. A. Metlitski and S. Sachdev, Phys. Rev. B **82**, 075128 (2010); New J. Phys. **12**, 105007 (2010).
 - [8] S. Sachdev and R. La Plata, Phys. Rev. Lett. **111**, 027202 (2013).
 - [9] See, for example, the analysis of incommensurate charge density waves by C. Castellani, C. Di Castro, and M. Grilli, Phys. Rev. Lett. **75**, 4650 (1995); F. Becca, M. Tarquini, M. Grilli, and C. Di Castro, Phys. Rev. B **54**, 12443 (1996); A. Perali, C. Castellani, C. Di Castro, and M. Grilli, Phys. Rev. B **54**, 16216 (1996).
 - [10] J.A. Hertz, Phys. Rev. B **14**, 1165 (1976).
 - [11] A.J. Millis, Phys. Rev. B **48**, 7183 (1993).
 - [12] A. Abanov, A. V. Chubukov, and J. Schmalian, Adv. Phys. **52**, 119 (2003); A. Abanov and A. V. Chubukov, Phys. Rev. Lett. **93**, 255702 (2004).
 - [13] B. L. Altshuler, L. B. Ioffe, and A. J. Millis, Phys. Rev. B **52**, 5563 (1995).
 - [14] D. Bergeron, D. Chowdhury, M. Punk, S. Sachdev, and A.-M. S. Tremblay, Phys. Rev. B **86**, 155123 (2012).
 - [15] Hot spots are points on the Fermi surface that are connected by the ordering wave vector \mathbf{Q} .
 - [16] F. Stern, Phys. Rev. Lett. **18**, 546 (1967).
 - [17] See, for example, L. Dell'Anna and W. Metzner, Phys. Rev. B **73**, 045127 (2006).
 - [18] C. Nayak and F. Wilczek, Nucl. Phys. B **417**, 359 (1994); **430**, 534 (1994).
 - [19] V. Oganessian, S. A. Kivelson, and E. Fradkin, Phys. Rev. B **64**, 195109 (2001).
 - [20] W. Metzner, D. Rohe, and S. Andergassen, Phys. Rev. Lett. **91**, 066402 (2003).
 - [21] M. A. Metlitski and S. Sachdev, Phys. Rev. B **82**, 075127 (2010).